# Cascading Failure Propagation Simulation in Integrated Electricity and Natural Gas Systems

Zhejing Bao, Qihong Zhang, Lei Wu, and Dawei Chen

Abstract—The sharp increase in the total installed capacity of natural gas generators has intensified the dynamic interaction between the electricity and natural gas systems, which could induce cascading failure propagation across the two systems that deserves intensive research. Considering the distinct time response behaviors of the two systems, this paper discusses an integrated simulation approach to simulate the cascading failure propagation process of integrated electricity and natural gas systems (IEGSs). On one hand, considering instantaneous re-distribution of power flows after the occurrence of disturbance or failure, the steady-state AC power flow model is employed. On the other hand, gas transmission dynamics are represented by dynamic model to capture the details of its transition process. The interactions between the two systems, intensified by energy coupling components (such as gas-fired generator and electricity-driven gas compressor) as well as the switching among the operation modes of compressors during the cascading failure propagation process, are studied. An IEGS composed of the IEEE 30-bus electricity system and a 14-node 15-pipeline gas system is established to illustrate the effectiveness of the proposed simulation approach, in which two energy sub-systems are coupled by compressor and gas-fired generator. Numerical results clearly demonstrate that heterogeneous interactions between electricity and gas systems would trigger the cascading failure propagation between the two coupling systems.

Index Terms—Cascading failure propagation, integrated electricity and natural gas system (IEGS), gas compressor, transmission dynamics.

#### I. INTRODUCTION

WITH the increasing installation of energy coupling components such as gas-fired generators and electricity-driven gas compressors, the electricity system has been coupled with the natural gas system more intensively, forming the integrated electricity and natural gas system (IEGS) [1], [2]. Specifically, gas-fired generators serve as power

Manuscript received: July 8, 2019; accepted: January 2, 2020. Date of Cross-Check: January 2, 2020. Date of online publication: June 29, 2020.

DOI: 10.35833/MPCE.2019.000455

sources in the electricity system and as gas loads in the gas system. Electricity-driven compressors installed along gas pipelines [3] can compensate for pressure losses due to transmission friction and/or heat transfer by consuming electric energy [4], [5]. Indeed, compressors can sustain pressures and facilitate the delivery of natural gas to load nodes, especially gas-fired electricity generation nodes. This is of crucial importance since gas-fired generators are more susceptible to pressure drops than other non-generation natural gas loads [6], [7].

The increasingly complicated interactions and interdependencies of the two distinct physical networks impose remarkable challenges on the reliable operation of IEGS [8], [9]. Intuitively, a local disturbance or failure in one system could propagate to the other and even reflect back to the original system through energy coupling components [3], [10], [11]. This dynamic interaction continues until a new operation state is reached.

Indeed, in IEGS, there are many types of interactions that can spread local disturbances or failures throughout the whole system [12]. For example, in severe weather situations, e.g., unusual chilly days, the demands for electricity and gas may peak together. The increasing gas demand can significantly elevate mass flow rates through compressors and simultaneously lower the inlet pressures at gas-fired generators. As a result, compressors need to consume more electric energy for maintaining the normal operation of gas-fired generators, which, along with the electricity demand peak, can further stress the power system operation [2], [9], [13], [14]. Similarly, when a local failure in the electricity system causes forced outage of compressors, inlet pressures at gasfired generators could gradually decrease. When pressures are lower than the threshold, electricity generators will be forced offline, leading to a further re-scheduling of electricity system. Consequently, it is imperative to investigate the cascading failure propagation procedure in the IEGS.

Existing researches on the IEGS have mainly focused on the interdependency analysis as well as the coordinated scheduling and planning. The unidirectional effect of intermittent wind generation on pressures fluctuations in gas pipelines has been studied in [15] by adopting gas dynamics equations, while the influence of variations of gas pressures, mass flow rates, and compressor electricity consumption on power flow re-distribution is not discussed. A quasi-dynamic simulation by extending the simulation tool SAInt has been developed to analyze the impact of the interdependence on



This work was supported by the National Natural Science Foundation of China (No. 51777182), and the National Natural Science Foundation (No. CMMI1635339). The authors would like to thank Mr. Zhewei Jiang of Zhejiang University, Hangzhou, China for helping prepare the revision of the manuscript.

This article is distributed under the terms of the Creative Commons Attribution 4.0 International License (http://creativecommons.org/licenses/by/4.0/).

Z. Bao, Q. Zhang, and D. Chen are with the College of Electrical Engineering, Zhejiang University, Hangzhou 310027, China (e-mail: zjbao@zju.edu.cn; zh\_qihong@zju.edu.cn; dwchen@zju.edu.cn).

L. Wu (corresponding author) is with the Department of Electrical and Computer Engineering, Stevens Institute of Technology, Hoboken, NJ 07901, USA (e-mail: lei.wu@stevens.edu).

supply security [10]. The impacts of interdependencies between electricity and natural gas systems in terms of security of energy supply have been analyzed in [16] via a steadystate gas flow model. A robust security-constrained unit commitment model is proposed to enhance operational reliability of IEGS against transmission line outages [17]. A long-term robust co-optimization planning model for IEGS is presented in [4] to minimize the total investment and operation costs. An interval optimization based operation strategy for IEGS considering demand response and wind uncertainty is proposed [18]. The optimal unit sizing for integrated energy system has been investigated, using multi-objective interval optimization and evidential reasoning approach [19]. A coordinated model of IEGS, formulated as a mixed-integer linear programming (MILP) problem, has been proposed to study the interdependence of electricity and natural gas transmission networks [20]. An analytical methodology has been developed to quantify operational flexibilities and restrictions that the gas system would introduce to the power system [21]. An MILP formulation to couple the electricity and gas systems has been investigated, accounting for gas adequacy to assure the power system reliability [22]. A robust scheduling model for the wind-integrated IEGS has been developed in [23] considering N-1 contingencies of both gas pipelines and electricity transmission lines.

However, to the best of the authors' knowledge, research on the cascading failure propagation procedure triggered by various interactions between electricity and natural gas systems is very limited. Specifically, the cascading failure propagation throughout the IEGS is very different from that in individual electricity or natural gas system, due to distinct physical characteristics of the electricity and natural gas systems as well as the operation mode switching of gas compressors during the propagation process. Thus, in order to discover the cascading evolution dynamics during the disturbance or failure propagation, this paper proposes an integrated co-simulation solution.

The major contributions of this work are twofold:

- 1) As an important energy coupling component, a natural gas compressor during the disturbance or failure induced transient process is modelled via four operation modes and their transition. The switching among operation modes is triggered when certain operation constraints are activated.
- 2) A unified co-simulation framework is proposed to discover the bi-directional interaction between electricity and natural gas systems, in which the models of gas transmission and power flow are combined via energy coupling components, such as gas-fired generators and electricity-driven gas compressors. In the co-simulation, considering the slow velocity of natural gas, a dynamic transmission model of the natural gas system is adopted. Meanwhile, the steady-state AC power flow model is applied owing to the instantaneous power flow re-distribution, and an economic power dispatching under failure propagation is included to derive reasonable results.

The remaining paper is organized as follows. The mechanism of cascading failure propagation and the integrated simulation framework of IEGS are presented in Section II. Sec-

tion III addresses the modelling of integrated simulation solution to describe the cascading failure propagation. Simulation results are presented in Section IV, and the conclusions are drawn in Section V.

#### II. MECHANISM AND CO-SIMULATION FRAMEWORK OF CASCADING FAILURE PROPAGATION IN IEGS

The operation of electricity and natural gas systems becomes increasingly interdependent, due to the intensified physical interconnection via energy coupling assets in both systems. The cascading failure propagation is a consequence of such interdependence and coupling. An illustrative schematic on the mechanism of cascading failure propagation between the two systems is depicted in Fig. 1, in which natural gas and electricity systems are denoted as A and B, respectively, while the interaction takes place through two energy coupling components.

Figure 1 describes a complicated bi-directional interaction between the two systems in the cascading failure propagation process. Assuming that the IEGS operates at an initial steady state, a disturbance or failure A1 occurs in system A, which induces the change in the input of energy coupling component 1. Coupling component 1 will respond to the variation in the input, which makes its output deviating from the initial value. This may lead to a consequent disturbance or failure B1 in system B, which can further result in the variation in the input of another energy coupling component 2. The corresponding change in the output of coupling component 2 would trigger another disturbance or failure in system A. Thus, the bi-directional interaction process can be understood as follows: the local disturbance or failure A1 in system A is the source of cascading failure propagation process; the disturbance B1 in system B is a consequence of disturbance A1 in system A; finally, B1 imposes a further impact on system A, by triggering a new disturbance or failure A2 in system A.

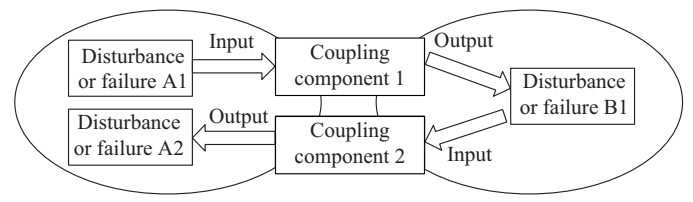


Fig. 1. Schematic illustration of cascading failure propagation mechanism in IEGS.

The time constants of dynamics in electricity and natural gas infrastructures vary from milliseconds to hours. That is, the transportation of the two types of energy occurs in different timeframes. Specifically, electric energy travels at the speed of light, while the velocity of natural gas delivery is typically low (10 m/s) [10]. Thus, after a disturbance or failure, electricity system may divert itself to a new operation state instantaneously, and consequently the steady-state model of electricity power flow is considered. On the contrary, in the gas system, the time evolution of mass flow rates and pressures after the occurrence of a disturbance or failure can-

not be neglected, and as a result, the dynamic model will be applied to capture dynamic behaviors of natural gas transmission, especially during the propagation process. In order to accurately describe the direct and indirect impacts of disruptions originating from one system and spreading to the other, the integrated co-simulation of gas and electric power systems needs to be implemented in a unified framework.

The proposed co-simulation framework is shown in Fig. 2. With known initial electricity demands, non-generation

gas demands, and gas source pressures, the optimal scheduling of electricity system considering steady-state power flow is implemented every  $\Delta t_p$  period. And during the time span between two consecutive electricity optimal scheduling, the dynamic natural gas flow calculation is conducted with a much shorter simulation step  $\Delta t_{g}$ . The alternating execution of electricity scheduling and natural gas flow calculation will cover the entire time evolution process, aiming to achieve an integrated co-simulation solution.

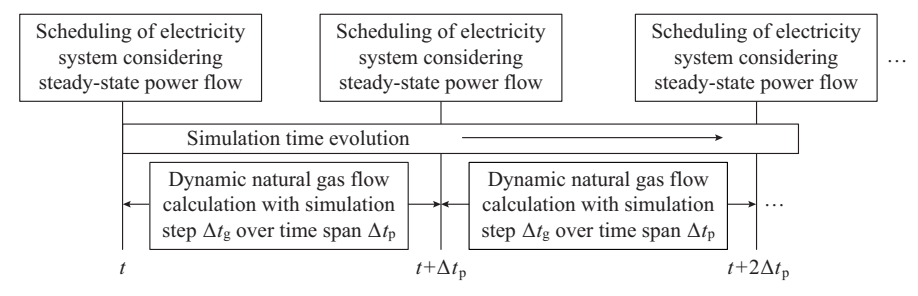


Fig. 2. Timeframe of integrated co-simulation solution to describe cascading failure propagation in IEGS.

# III. MODELLING OF INTEGRATED CO-SIMULATION SOLUTION DESCRIBING CASCADING FAILURE PROPAGATION

#### A. Modelling of Energy Coupling Components

The electricity and natual gas systems are physically interconnected via a number of assets. In this study, two of the most significant energy coupling assets interconnecting the two systems are considered, i. e., electricity-driven natural gas compressors and gas-fired electricity generators.

Natural gas compressors are installed along pipelines in order to compensate pressure losses. Maintaining the pressures of natural gas flows by compressors requires the consumption of electric power. The electric power consumption  $P_c(t)$ of a compressor is given by:

$$P_{c}(t) = f \frac{\kappa}{\kappa - 1} \frac{RTZ\rho_{n}}{K_{1}} M_{c}(t) \left[ \left( \frac{\pi_{out}(t)}{\pi_{in}(t)} \right)^{\frac{\kappa - 1}{\kappa}} - 1 \right]$$
 (1)

where  $M_c(t)$  is the mass flow rate through a compressor;  $\pi_{out}(t)$  and  $\pi_{in}(t)$  are the pressures at the outlet and inlet of a compressor, respectively;  $\kappa = 1.3$  is the isentropic coefficient of natural gas;  $\rho_n$  is the gas density at reference conditions;  $K_1$  is the product of adiabatic efficiency of compressor and the driver efficiency; gas constant R = 500; temperature T =273 K; compressibility factor Z = 0.9; and f is the fraction of total driver power provided by electric drivers. All the other parameters are empirical parameters of compressors, which can be referred to [10]. Equation (1) indicates that the electric power consumption is determined by the pressure ratio between suction and discharging as well as mass flow rate

The natural gas mass flow rate running through a compressor with the pressure lifting is constrained by:

$$M_c^{\min} \le M_c(t) \le M_c^{\max} \tag{2}$$

where  $M_c^{\min}$  and  $M_c^{\max}$  are the lower and upper limits of mass

flow rate through it, respectively.

The pressure ratio is also limited within a feasible range as in (3), which is based on compressor characteristics:

$$PR_{\min} \le \frac{\pi_{out}(t)}{\pi_{in}(t)} \le PR_{\max} \tag{3}$$

where  $PR_{\min}$  and  $PR_{\max}$  are the lower and upper limits of pressure ratio between the outlet and inlet, respectively.

The pressure at the outlet of a compressor  $\pi_{out}(t)$  is also constrained by:

$$\pi_{out}^{\min} \le \pi_{out}(t) \le \pi_{out}^{\max}$$
 (4)

 $\pi_{out}^{\min} \leq \pi_{out}(t) \leq \pi_{out}^{\max} \tag{4}$  where  $\pi_{out}^{\min}$  and  $\pi_{out}^{\max}$  are the lower and upper limits of outlet pressure, respectively.

The natural gas compressor is commonly described via the following four operation modes:

- 1) Mode 1: fixed inlet mass flow rate.
- 2) Mode 2: fixed boost ratio  $\pi_{out}(t)/\pi_{in}(t)$ .
- 3) Mode 3: fixed outlet pressure.
- 4) Mode 4: acting as a regular pipeline.

Indeed, in Mode 4, the compressing function does not work and the compressor acts as a regular pipeline. This mode could be triggered when the electricity supplied to compressor is insufficient or the mass flow rate through it becomes a negative value, i.e., running from outlet to inlet, based on the assumption that the compressed mass flow is uni-directional.

The switching among four operation modes is illustrated in Fig. 3 with three dimensions, i.e., mass flow rate, pressure ratio, and outlet pressure. Specifically, ① in the normal operation, the compressor usually works in Mode 1, denoted by point A; 2 the occurrence of a disturbance forces the operation point to move from A to B, while during the process, it still operates in Mode 1 with the fixed mass flow rate; 3 once completely moved to point B, the pressure ratio reaches its upper limit, and the operation mode switches from Mode 1 to Mode 2; (4) from point B, the operation point adjusts to C, maintaining the maximum pressure ratio; (5) at point C, the upper limit of outlet pressure is reached, and the operation mode transits from Mode 2 to Mode 3; 6 in Mode 3, the operation point moves from C to D, with the outlet pressure at its upper limit; (7) when the operation point goes from D to E, the mass flow rate through the compressor falls under the lower limit of the compressed mass flow rate, and the operation mode changes from Mode 3 to Mode 4, i.e., the compressor works as a regular pipeline. In summary, the disturbance or failure can lead to the operation point of compressor switching from A all the way to E, while its operation mode switches from Mode 1 to Mode 4 through Mode 2 and Mode 3. In addition, during the failure evolution procedure, certain compressor operation limits might be activated which trigger the switching of operation modes.

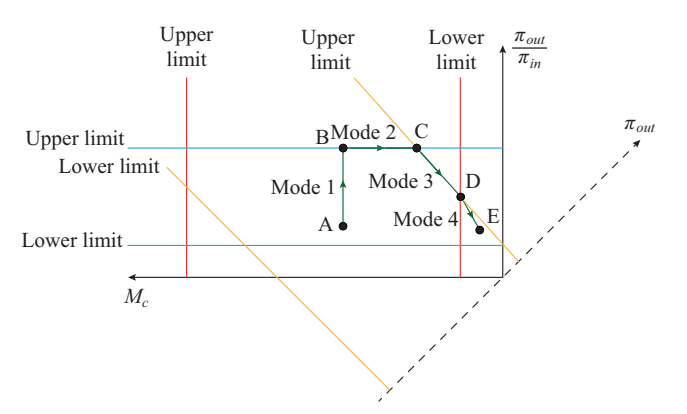


Fig. 3. Operation mode switching of a natural gas compressor.

As another energy coupling component, a gas-fired electricity generator connects the electricity and natural gas system by consuming natural gas to generate electricity. The relationship between natural gas consumption and the electricity generation can be formulated as follows:

$$M_{gas,e}(t) = \alpha P_{gas,e}(t) \tag{5}$$

where  $M_{gas,e}(t)$  is the mass flow rate of natural gas consumption to generate electricity at the level of  $P_{gas,e}(t)$ ; and  $\alpha$  is the constant energy conversion coefficient.

In addition, the operation constraints on the pressure at the inlet of gas-fired generator are usually imposed, which will be presented in the following section when modelling gas transmission dynamics.

# B. Modelling of Power Dispatching Considering AC Power Flow

The steady-state AC power flow model is adopted to simulate the impacts of a disturbance on the power grid, including instantaneous re-distribution of power flows as well as reactive power and bus voltage. Constraints of the AC power flow model are described as follows.

# 1) Power flow constraint

$$P_i(t) = V_i(t)V_i(t)(G_{ii}\cos\theta_{ii}(t) + B_{ii}\sin\theta_{ii}(t))$$
 (6)

$$Q_i(t) = V_i(t)V_i(t)(G_{ii}\sin\theta_{ii}(t) - B_{ii}\cos\theta_{ii}(t))$$
 (7)

where  $P_i(t)$  and  $Q_i(t)$  are the active and reactive power injec-

tions at bus i at time t, respectively;  $V_i(t)$  is the amplitude of the voltage at bus i at time t;  $\theta_{ij}(t) = \theta_i(t) - \theta_j(t)$  is the difference in phase-angles of the voltages at bus i and bus j at time t; and  $Y_{ij} = G_{ij} + \mathrm{j}B_{ij}$  is defined as the admittance of the system.

#### 2) Generator Output Constraint

$$P_{gi}^{\min} \le P_{gi}(t) \le P_{gi}^{\max} \quad i \in G$$
 (8)

$$Q_{gi}^{\min} \le Q_{gi}(t) \le Q_{gi}^{\max} \quad i \in G$$
 (9)

where  $P_{gi}(t)$  and  $Q_{gi}(t)$  are the active and reactive power outputs of generator i, respectively;  $P_{gi}^{\max}$ ,  $P_{gi}^{\min}$ ,  $Q_{gi}^{\max}$ , and  $Q_{gi}^{\min}$  are the corresponding upper and lower limits of  $P_{gi}(t)$  and  $Q_{gi}(t)$ , respectively.

### 3) Bus Voltage Constraint

$$V_i^{\min} \le V_i(t) \le V_i^{\max} \tag{10}$$

where  $V_i^{\text{max}}$  and  $V_i^{\text{min}}$  are the upper and lower limits of bus voltage  $V_i(t)$ , respectively.

# 4) Branch Capacity Constraint

$$-F_b^{\max} \le F_b(t) \le F_b^{\max} \tag{11}$$

where  $F_b(t)$  is the power transferred through branch b; and  $F_b^{\text{max}}$  is the capacity of branch b.

In actual grid operation, load shedding is considered as the last resort to ensure system security. Constraint (12) is included to consider load shedding in the economic dispatch model.

$$0 \le P_{li}(t) \le P_{li}^0 \quad i \in L \tag{12}$$

where  $P_{li}(t)$  is the electricity load at time t;  $P_{li}^0$  is the original electricity load at bus i before load shedding; and L is the set of electricity load.

The dispatching objective in electricity system usually targets on minimizing the total operation costs, including generation cost and load shedding cost:

$$\min \sum_{i \in G} [c_{gi}(t) P_{gi}(t) + c_{li}(t) (P_{li}^{0} - P_{li}(t))]$$
(13)

where  $c_{gi}(t)$  is the price coefficient for electricity generator j; and  $c_{li}(t)$  is the price coefficient of load shedding at load i. Usually,  $c_{li}(t)$  is much higher than  $c_{gi}(t)$ , indicating that load shedding is the last resort for maintaining system security. In the simulation,  $c_{li}(t)$  for electricity-driven compressor is identical to that for other electricity loads, i.e., they are given the same priority for load shedding, while the optimal load shedding strategy will drive the minimum system losses.

The optimization problem composed by objective (13) and constraints (6)-(12) can be solved by particle swarm optimization (PSO). In PSO, AC power flow is calculated by Newton-Raphson iteration, the constraints (8), (9) and (12) are satisfied in particle generations, and the constraints (10) and (11) are satisfied by imposing penalty on the optimization objective.

#### C. Modelling of Natural Gas Transmission Dynamics

In natural gas system, the travelling time of natural gas mass from source nodes to load nodes is not negligible. Indeed, after the occurrence of a disturbance or failure, the gas system would take a much longer response time to reach a new steady state. Thus, during the transient propagation pro-

cess, gas dynamic model has to be used to describe such transmission characteristics.

In order to represent the dynamic characteristics of natural gas system accurately, the basic principles of fluid dynamics is used to describe natural gas transmission along pipelines. The mass-balance equation is formulated as follows, describing the conservation of natural gas mass in a pipeline [24]:

$$\frac{\partial \rho}{\partial t} + \frac{\partial M}{A \partial x} = 0 \tag{14}$$

where  $\rho$  and M are the density and mass flow rate of natural gas, respectively; t and x are the time and spatial indices, respectively; and A is the cross-sectional area of the pipeline.

In the theory of natural gas transmission dynamics, the momentum equation, also known as Navier-Stokes equation, is used to represent the momentum transport in the continuum of natural gas. With proper assumptions, the equation can be simplified as the following form [24]:

$$\frac{\partial M}{A\partial t} + \frac{\partial \pi}{\partial x} + \frac{\lambda}{2d} \frac{M^2}{\rho A^2} = 0 \tag{15}$$

where d is the diameter of the pipeline. The value of friction factor  $\lambda$  is usually chosen as 0.015. The relationship between pressure  $\pi$  and density  $\rho$  can be expressed as  $\pi = c^2 \rho$ , where parameter  $c^2 = RTZ$ . It is noteworthy that fluid dynamics constraints (14) and (15) are partial differential equations, and their solutions can be approximated by the Wendroff difference method. Consequently, (14) and (15) can be reformulated as (16) and (17), describing the dynamic characteristics of natural gas mass flow rates and pressures at two nodes m and n of a pipeline mn. It can be seen that considering transmission dynamics, the mass flow rates and pressures of natural gas within a pipeline are coupled in space and time.

$$\pi_{n}(t+(l+1)\Delta t) + \pi_{m}(t+(l+1)\Delta t) - \pi_{n}(t+l\Delta t) - \pi_{m}(t+l\Delta t) + \frac{\Delta t c^{2}}{L_{mn}A_{mn}} [M_{n}(t+(l+1)\Delta t) - M_{m}(t+(l+1)\Delta t) + M_{n}(t+l\Delta t) - M_{m}(t+l\Delta t)] = 0 \quad l = 0, 1, ..., N_{t} - 1$$

$$\frac{1}{A_{mn}} [M_{n}(t+(l+1)\Delta t) + M_{m}(t+(l+1)\Delta t) - M_{n}(t+l\Delta t) - M_{n}(t+l\Delta t)] + \frac{\Delta t}{L_{mn}} [\pi_{n}(t+(l+1)\Delta t) - \pi_{m}(t+(l+1)\Delta t) + \pi_{n}(t+l\Delta t)] + \frac{\lambda \Delta t \varpi_{mn}}{4d_{mn}A_{mn}} [M_{n}(t+(l+1)\Delta t) + M_{m}(t+(l+1)\Delta t) + M_{m}(t+(l+1)\Delta t) + M_{m}(t+(l+1)\Delta t) + M_{m}(t+(l+1)\Delta t) + M_{m}(t+l\Delta t)] = 0$$

$$l = 0, 1, ..., N_{t} - 1$$

$$(16)$$

where  $L_{mn}$  is the length of pipeline mn;  $N_t$  is the number of steps to simulate gas dynamics during an execution period of electricity scheduling, and is equal to  $\Delta t_p/\Delta t_g$ ; and  $\varpi_{mn}$  is the average gas flow rate, which is calculated as  $\varpi_{mn} = c^2 (M_m(t)/\pi_m(t) + M_n(t)/\pi_n(t))/(2A_{mn})$ .

In addition, in natural gas system, at an intersection where nodes  $m, m+1, \dots, mm$  are connected, a consensus gas pressure as well as a balanced mass flow rate needs to be guaranteed. Such boundary conditions are imposed as follows:

$$\pi_m(t+(l+1)\Delta t) = \pi_{m+1}(t+(l+1)\Delta t) = \dots =$$

$$\pi_{mm}(t+(l+1)\Delta t) \quad l = 0, 1, \dots, N_t - 1$$
(18)

$$M_m(t+(l+1)\Delta t) + M_{m+1}(t+(l+1)\Delta t) + \dots + M_{mm}(t+(l+1)\Delta t) = 0 \quad l = 0, 1, \dots, N_t - 1$$
 (19)

In the natural gas system, the mass flow rates at generation and non-generation gas load nodes,  $M_n(t+(l+1)\Delta t)$ , l=0,1,...,  $N_t-1,n\in GL\cup NGL$  (GL and NGL are the sets of generation and non-generation natural gas load nodes, respectively), are known during the time span of gas dynamics simulation. The mass flows and pressures also need to satisfy their upper and lower operation limits given in (20) and (21), respectively. Constraint (21) also includes limits on natural gas pressures at inlet of gas-fired generators.

$$-M_m^{\max} \le M_m (t + (l+1)\Delta t) \le M_m^{\max} \quad l = 0, 1, ..., N_t - 1 \quad (20)$$

$$\pi_m^{\min} \le \pi_m (t + (l+1)\Delta t) \le \pi_m^{\max} \quad l = 0, 1, ..., N_t - 1$$
(21)

When considering the natural gas transmission dynamics, (16)-(21) constitute an LP problem, which can be effectively solved by commercial LP solvers such as CPLEX to determine the pressures  $\pi_{m(n)}(t+(l+1)\Delta t)$  and the mass flow rates  $M_{m(n)}(t+(l+1)\Delta t), l=0,1,...,N_t-1$  at the two nodes m and n of each pipeline.

# D. Procedure of Cascading Propagation Simulation

The procedure of the integrated co-simulation for cascading failure propagation in IEGS is described as follows.

Step 1: at t=0, calculate initial steady state of the electricity and natural gas system. Assuming that the compressor operates in Mode 1 with the given inlet mass flow rate, calculate the initial steady-state operation point of the natural gas system by the steady-state model [25], with the initial values of generation and non-generation gas demands as well as the pressures of gas source nodes. With the compressor electricity demand, implement electricity dispatching optimization (6)-(13) to derive the initial steady state of the electricity system.

Step 2: initiate a cascading propagation by starting a triggering event.

Step 3: conduct power dispatching optimization (6)-(13) to derive a new electricity steady state in terms of generations and loads, when AC power flow calculation converges.

Step 4: derive natural gas consumptions of gas-fired generators via (5) and on/off state of electricity-driven natural gas compressors.

Step 5: perform the simulation of natural gas transmission dynamics over the following  $\Delta t_p$  time period. In the simulation of gas dynamics, switching among the four operation modes of natural gas compressor is achieved by checking whether the pressure ratio, outlet pressure, or mass flow rate reaches the corresponding limit.

Step 6: calculate the electricity consumption of natural gas compressor via (1).

Step 7: set  $t = t + \Delta t_p$  and go to Step 3 if the cascade still keeps spreading till the operation states of the IEGS remain unchanged, i. e., a new steady state of the entire IEGS is achieved.

During the co-simulation procedure of cascading failure propagation, if a disturbance or failure occurs, i.e., the variation of electricity or natural gas demand, or the outage of an electricity branch or a gas pipeline, it will be considered in the corresponding power dispatching in *Step 3* or the computation of natural gas transmission dynamics in *Step 5*.

In summary, in a unified time frame, different time scales are used to alternately solve the two models, i.e., natural gas transmission dynamics model and AC power flow based electricity dispatching model, to simulate the disturbance or failure propagation process between the two coupled systems.

#### IV. CASE STUDIES

An IEGS is established to explore the disturbance or failure propagation process, which consists of a 14-node 14branch natural gas system and the IEEE 30-bus electricity system, as shown in Fig. 4. The natural gas system includes 2 sources at nodes 1 and 12, 3 non-generation sinks at nodes 9-11, and 1 gas-fired generator GG at node 7. The gas-fired generator, as an energy coupling component, is also located at bus 2 in the electricity system. Besides the gas-fired generator, there are diesel generators DG1-DG5 in the electricity system. As shown in Fig. 4, the natural gas and electricity systems are coupled by the gas-fired generator and the electricity-driven compressor. In the natural gas system, the length of all pipelines is set as 1 km, except the one between nodes 8 and 13 which is 15 km. Consequently, a compressor is installed between nodes 13 and 14 to boost gas pressure, aiming to compensate for pressure losses due to the long-distance natural gas transmission.

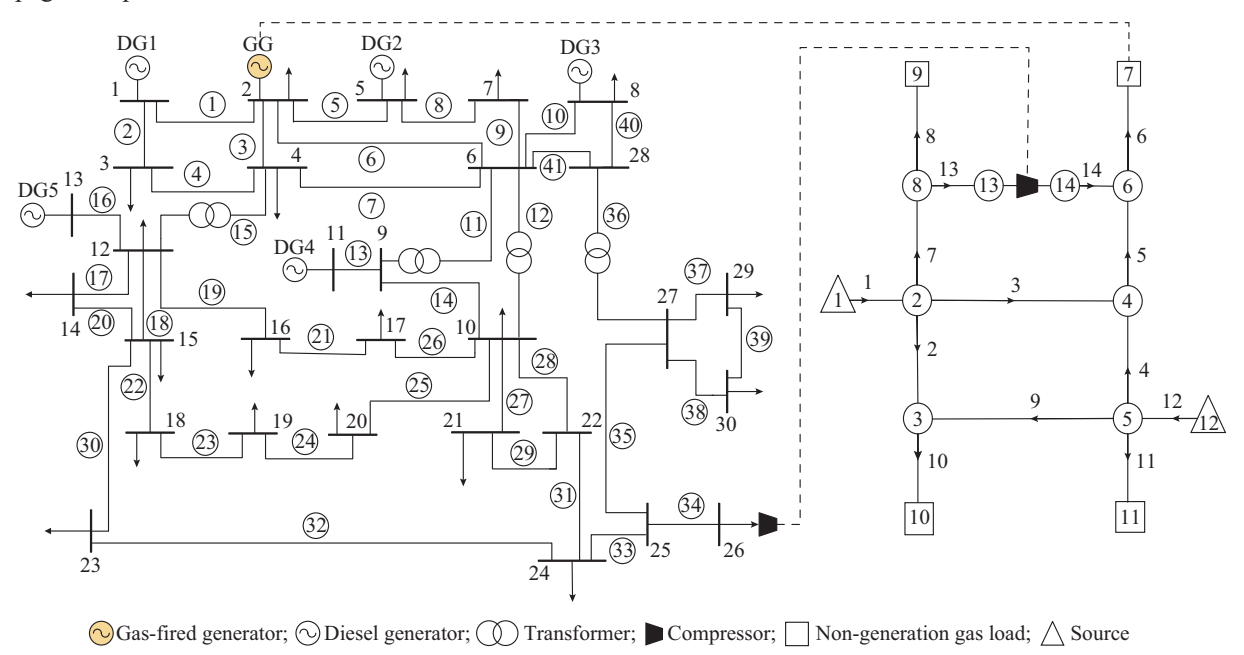


Fig. 4. Topologies of electricity and natural gas systems in IEGS.

## A. Case 1

In the simulation, the parameters are set as  $\Delta t_{\rm g} = 2$  s and  $\Delta t_{\rm p} = 10$  s. We consider that the IEGS initially operates at a steady-state point as described in Tables I-IV.

The compressor works in Mode 1 with the fixed mass flow rate of 3 kg/s, and the pressure ratio between outlet and inlet is 1.774. For the compressor, the limits on pressure ratio, outlet pressure, and compressed mass flow rate are set as [1, 1.9], [0.0344, 0.0907]MPa, and [0, 20]kg/s, respectively. And as a common pipeline in Mode 4, the reversed mass flow rate through it is constrained by [-20, 0)kg/s. The pressure at inlet of gas-fired generator is limited within [0.0425, 0.0638]MPa. In addition, during the disturbance propagation, the two natural gas sources operate under the constant pressure and variable mass flow rate (CP-VR) strategy, with the fixed pressure 0.0927 MPa and 0.0613 MPa, imposed on nodes 1 and 12, respectively.

In Case 1, it is assumed that at t = 600 s, the step increas-

es by 50% of the present values occur simultaneously in nongeneration gas demands at nodes 9-11, which is shown in Fig. 5. With the CP-VR strategy, the mass flow rates from the two sources increase significantly as a response to the increase in gas demands, while the increase in gas supply shows a little delay because of slow gas transmission dynamics.

 ${\bf TABLE~I}$  Initial Steady-state Values of Natural Gas Pressures at Nodes

Node	Pressure (MPa)	Node	Pressure (MPa)
1	0.0927	8	0.0392
2	0.0612	9	0.0267
3	0.0588	10	0.0473
4	0.0610	11	0.0541
5	0.0612	12	0.0812
6	0.0601	13	0.0353
7	0.0532	14	0.0626

 ${\bf TABLE~II}$  Initial Steady-state Values of Mass Flow Rates Through Pipelines

Pipeline	Mass flow rate (kg/s)	Pipeline	Mass flow rate (kg/s)
1	11.6620	8	5.0000
2	2.9408	9	3.0592
3	0.7212	10	6.0000
4	1.1138	11	5.0000
5	1.8350	12	9.1730
6	4.8350	13	3.0000
7	8.0000	14	3.0000

TABLE III
INITIAL STEADY-STATE VALUES OF ACTIVE POWER FLOW THROUGH
BRANCHES

Branch	Power (MW)	Branch	Power (MW)	Branch	Power (MW)	Branch	Power (MW)
1	-3.2380	12	-0.9920	23	-0.3137	34	-0.3510
2	-2.6922	13	2.6895	24	0.6377	35	0.1782
3	-2.2855	14	-3.4540	25	-0.8577	36	-1.5104
4	-2.4445	15	-2.1367	26	-0.4823	37	-0.6109
5	-4.5809	16	2.5365	27	-1.6719	38	-0.6929
6	-2.6691	17	-0.8482	28	-0.8254	39	-0.3671
7	-1.8293	18	-1.8823	29	0.0781	40	-0.6103
8	1.1623	19	-0.7719	30	-0.6381	41	-0.9001
9	-3.4423	20	-0.2257	31	-0.7381		
10	1.6373	21	-0.4177	32	-0.3129		
11	-0.7645	22	-0.6349	33	-0.1783		

 $\label{total loss} TABLE\ IV$  Initial Steady-state Values of Net Injection Power at Buses

Bus	Power (MW)	Bus	Power (MW)	Bus	Power (MW)
1	5.9962+2.4889i	11	2.6895+2.9667i	21	-1.7500-1.1200i
2	6.4640-1.2701i	12	-1.1200-0.7500i	22	0
3	-0.2400-0.1200i	13	2.5365+3.5928i	23	-0.3200-0.1600i
4	-0.7600-0.1600i	14	-0.6200-0.1600i	24	-0.8700-0.6700i
5	-5.7360+0.3504i	15	-0.8200-0.2500i	25	0
6	0	16	-0.3500-0.1800i	26	-0.3671
7	-2.2800-1.0901i	17	-0.9000-0.5800i	27	0
8	2.2500+0.3740i	18	-0.3200-0.0900i	28	0
9	0	19	-0.9500-0.3400i	29	-0.2400-0.0900i
10	-0.5800-0.2000i	20	-0.2200-0.0700i	30	-1.0600-0.1900i

Figure 6 further shows that, during the process of natural gas source increase, due to unbalanced supply and demand of mass flow rates, the average pressures in the natural gas system decrease.

As for the compressor, the pressure ratio between the outlet and inlet is depicted in Fig. 7, where the compress ratio increases rapidly to mitigate the pressure decline caused by the initial triggering event. At t=608 s, the compress ratio reaches its upper limit and its operation mode is switched from Mode 1 to Mode 2. After the switching of the working modes of the compressor, the outlet pressure of gas-fired

generator still falls gradually. Finally, the gas-fired generator is off at t=752 s, because the inlet gas pressure falls below its lower bound, and the mass flow rate delivered to it becomes zero as shown in Fig. 5. Since the generation gas demand at node 7 is shed, the mass flow rates from the two sources decrease and the average pressures in the natural gas system upswing shown in Figs. 5 and 6.

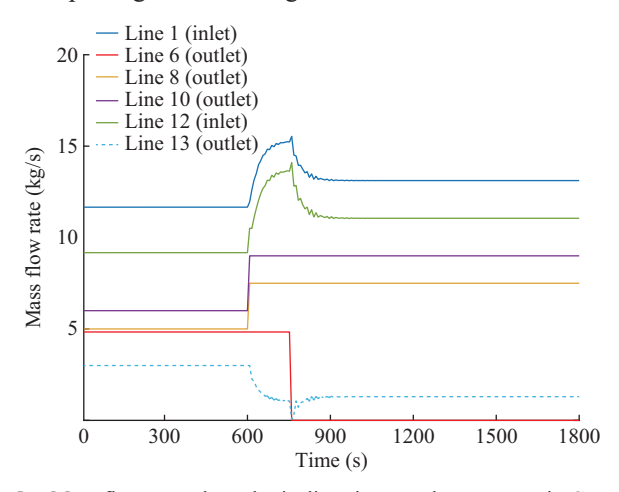


Fig. 5. Mass flow rates through pipelines in natural gas system in Case 1.

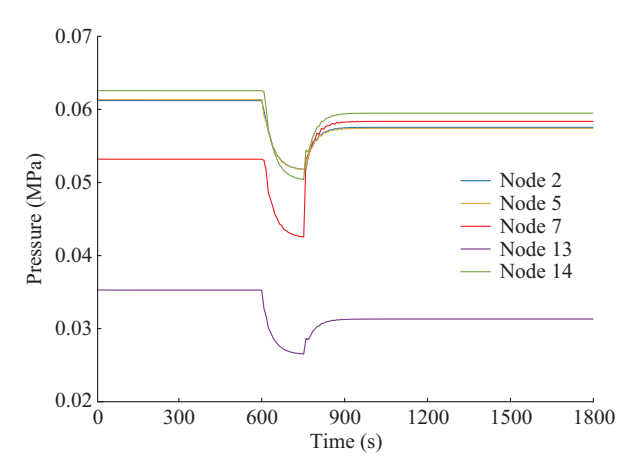


Fig. 6. Pressures at nodes in natural gas system in Case 1.

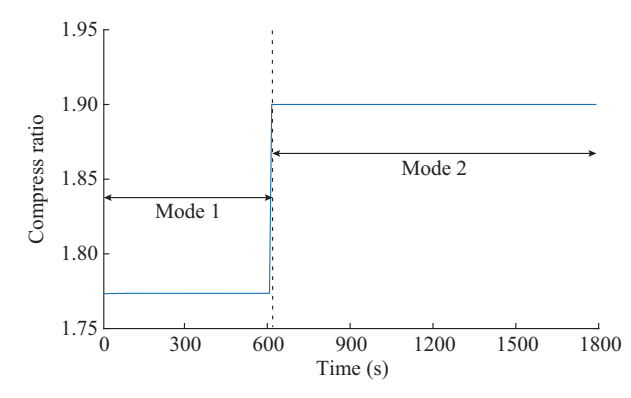


Fig. 7. Outlet/inlet pressure ratio and working mode of natural gas compressor in Case 1.

During the period from t = 608 s to t = 752 s, the electricity demand from the gas compressor varies with the change of compress ratio or mass flow rate, which induces fluctua-

tions in active power flows through electricity branches, as shown in Fig. 8. After t = 752 s, due to the offline of the gas-fired generator, all electricity demands are supplied by the other 5 diesel generators and power flow re-distribution is induced.

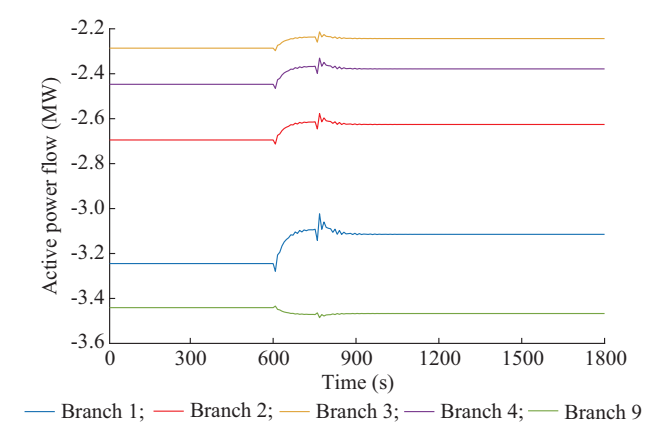


Fig. 8. Active power flows through branches in electricity system in Case 1.

In summary, the propagation process can be divided into two periods. During the first period from t=600 s to t=752 s, a triggering event of non-generation gas demand increase causes the pressure drop, the increase of compress ratio, and power flow fluctuations. During the second period after t=752 s, the inlet pressure drop forces the gas-fired generator offline and in turn causes the power flow re-distribution. After the transient process, the IEGS completes the transition from an initial steady state to a new one.

#### B. Case 2

In Case 2, the propagation process between the electricity and natural gas systems is investigated, initiated by the outage of natural gas pipeline 5 at t=600 s. Since the failure occurs on gas pipeline 5, the outlet pressure of gas-fired generator falls rapidly and soon falls below its lower bound at t=624 s, inducing the outage of gas-fired generator. And the mass flow rate at outlet of pipeline 6 becomes zero, as shown in Fig. 9.

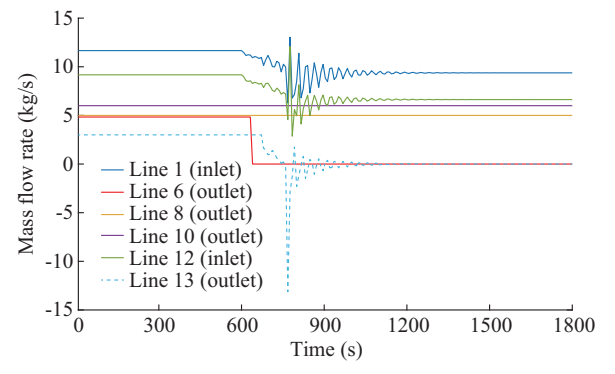


Fig. 9. Mass flow rates through pipelines in natural gas system in Case 2.

After the outage of the gas-fired generator, the pressures at nodes 6, 7 and 14 upswing rapidly. On the contrary, the inlet pressure of the compressor at node 13 rises gradually because of the slow gas transmission dynamics, which is

shown in Fig. 10.

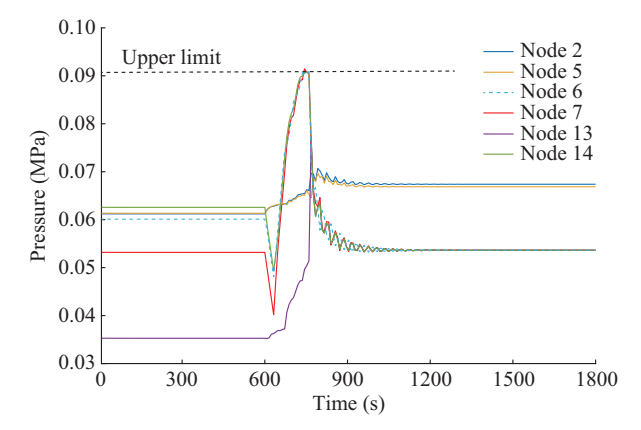


Fig. 10. Pressures at nodes in natural gas system in Case 2.

The compress ratio variation and working mode switching during the propagation are illustrated in Fig. 11. After a temporary descent, the sharp lift of pressure at compressor outlet leads to a significant increase in compress ratio. During 600-672 s, the compressor still works in Mode 1 with the fixed mass flow rate 3 kg/s. As the compress ratio keeps increasing, it reaches the upper limit 1.9 at t = 672 s. During the period 672-736 s, the compressor works in Mode 2 with the compress ratio fixed at 1.9, and meanwhile, the outlet pressure goes up continuously. At t = 736 s, the outlet pressure of compressor reaches its upper limit 0.0907 MPa, and then its working mode is switched from Mode 2 to Mode 3. At t = 760 s, the mass flow rate through compressor reverses due to the outage of gas-fired generator, and the compressor is forced to Mode 4. After t = 760 s, the compressor is forced off and regarded as a gas pipeline, and then the mass flow rate through it tends to be zero after a slow dynamic process because there is no natural gas demand at its downstream nodes. The working mode variations of compressor induce power flow variation, as shown in Fig. 12.

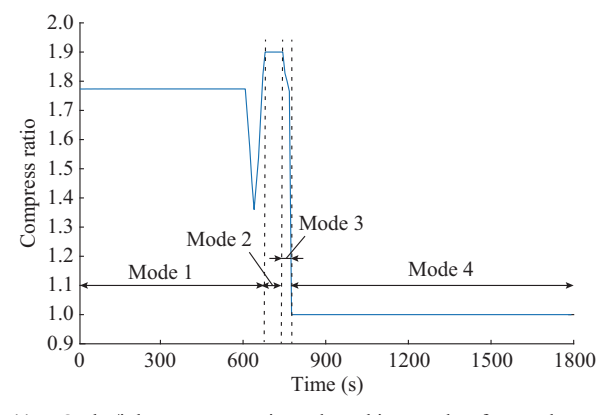


Fig. 11. Outlet/inlet pressure ratio and working mode of natural gas compressor in Case 2.

#### C. Case 3

At t = 600 s, the electricity branch 33 encounters an outage, and a new electricity steady state is instantaneously achieved by re-dispatching, as shown in Fig. 13. The power supply from the gas-fired generator changes from 8.634 MW

to 5.507 MW. Indeed, due to the capacity limit through electricity branch, some power loads including the load at bus 26 are partly shed. Thus, the power supply to the compressor is insufficient; and consequently, the compressor is forced to be in Mode 4 as shown in Fig. 14. The variation of power output from gas-fired generator leads to a conspicuous change of gas consumption, from 4.835 kg/s to 3.084 kg/s as shown in Fig. 15.

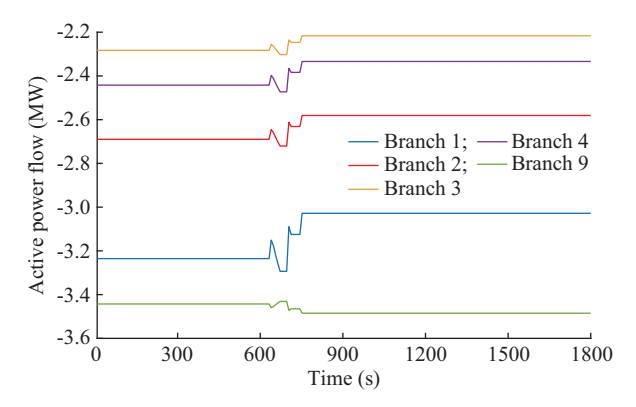


Fig. 12. Active power flows through branches in electricity system in Case 2.

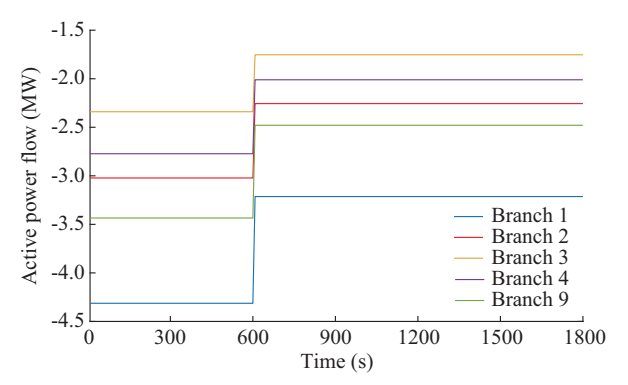


Fig. 13. Active power flows through branches in electricity system in Case 3.

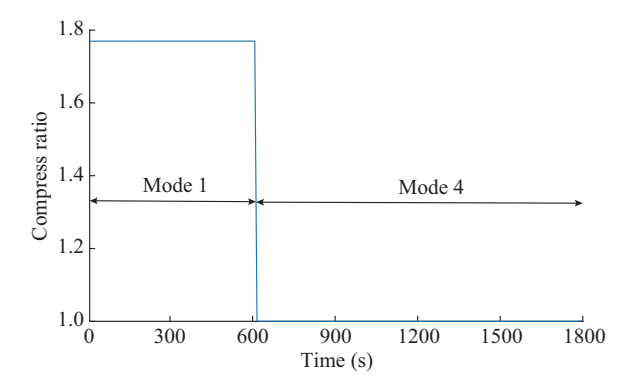


Fig. 14. Outlet/inlet pressure ratio and working mode of natural gas compressor in Case 3.

As shown in Fig. 15, after t = 600 s, the mass flow rates from two natural gas sources decrease significantly due to the reduction of mass flow rate delivered to the gas-fired generator. The average pressures in gas system increase to mitigate the unbalance of gas supply and demand during the slow transient process, as shown in Fig. 16.

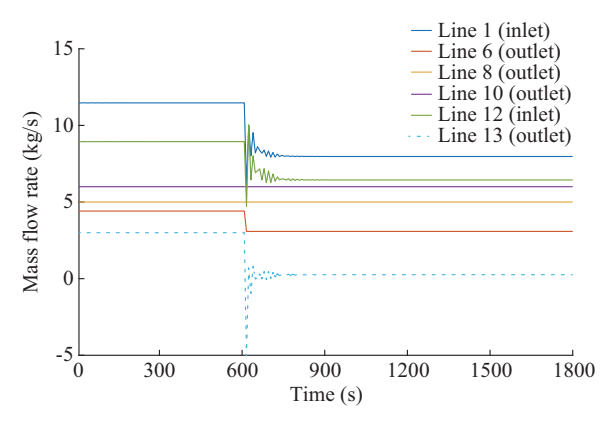


Fig. 15. Mass flow rates through pipelines in natural gas system in Case 3.

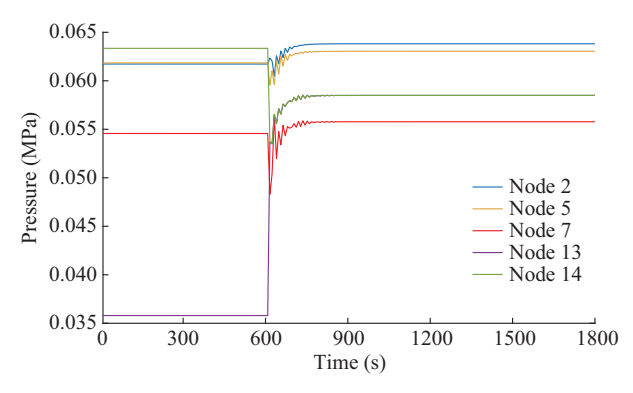


Fig. 16. Pressures at nodes in natural gas system in Case 3.

#### D. Discussion

The disturbance in the natural gas system such as non-generation gas demand variations, pipeline outage as well as induced changes of mass flow rates or pressures, can bring about a slow gas dynamic process and propagate to the electricity system through coupling components after a transient period, not instantaneously. On one hand, the increase in electricity demand of compressors can influence the operation points of the electricity system, but this influence is not significant due to the relatively small proportion of electricity consumptions of compressors in the total demand. On the other hand, the decrease in inlet pressure of gas-fired generators can lead to forced outages of gas-fired generators, which could vary the operation points of the electricity system significantly and even cut off some electricity loads, especially when certain branches are heavily loaded.

The re-distribution of power flows induced by the disturbance or failure in the electricity system is achieved instantaneously. It propagates from the electricity system to the natural gas system through electricity-driven natural gas compressors and/or gas-fired generators. Generator outages might lead to negligible impact on the network operation, owing to the small proportion of generation gas demand in the total gas demand and the flexibility of linepack within pipeline infrastructure. On the contrary, compressor outages would cause sharp and immediate decline of pressures at its downstream nodes including the inlet pressure of generator, which in turn forces the offline of gas-fired electricity generators.

#### V. CONCLUSION

This paper investigates the disturbance or failure induced cascading propagation process in the IEGS with energy coupling components, including gas-fired generators and electricity-driven natural gas compressors. An integrated simulation approach is proposed to describe the cascading failure propagation by integrating gas transmission dynamics and AC power flow based electricity optimal dispatching in a unified co-simulation framework, in which distinct time responses of the two systems are represented and the working mode switching of gas compressors is considered. Numerical case studies are implemented to illustrate the cascading propagation triggered via various interactions. Specifically, the disturbance of gas demand variation or gas pipeline outage can induce a slow propagation from the natural gas system to the electricity system. Meanwhile, compressor outage can lead to an immediate offline of gas-fired generators, which could bring about load shedding in the electricity system, especially when the electricity system is stressed. Consequently, it is suggested that special attentions need to be paid to maintain the normal operation of compressors. In addition, facing the slow propagation, prevention measures may be effective, which will be explored in our future research work.

#### REFERENCES

- [1] D. Chen, Z. Bao, and L. Wu, "Integrated coordination scheduling framework of electricity-natural gas systems considering electricity transmission N-1 contingencies and gas dynamics," *Journal of Modern Power Systems and Clean Energy*, vol. 7, no. 6, pp. 1422-1433, Nov. 2019.
- [2] A. Nikoobakht, J. Aghaei, M. Shafie-khah et al., "Continuous-time cooperation of integrated electricity and natural gas systems with responsive demands under wind power generation uncertainty," *IEEE Transactions on Smart Grid*, vol. 11, no. 4, pp. 3156-3170, Jul. 2020.
  [3] C. Liu, M. Shahidehpour, and J. Wang, "Coordinated scheduling of
- [3] C. Liu, M. Shahidehpour, and J. Wang, "Coordinated scheduling of electricity and natural gas infrastructures with a transient model for natural gas flow," *Chaos*, vol. 21, no. 2, pp. 1-12, Jun. 2011.
- [4] C. He, L. Wu, T. Liu et al., "Robust co-optimization planning of interdependent electricity and natural gas systems with a joint N-1 and probabilistic reliability criterion," *IEEE Transactions on Power Sys*tems, vol. 33, no. 2, pp. 2140-2154, Mar. 2018.
- tems, vol. 33, no. 2, pp. 2140-2154, Mar. 2018.

  [5] M. Moein, A. Ali, F. Mahmud et al., "A decomposed solution to multiple-energy carriers optimal power flow," *IEEE Transactions on Power Systems*, vol. 29, no. 2, pp. 707-716, Mar. 2014.

  [6] C. Liu, M. Shahidehpour, Y. Fu et al., "Security-constrained unit com-
- [6] C. Liu, M. Shahidehpour, Y. Fu et al., "Security-constrained unit commitment with natural gas transmission constraints," *IEEE Transactions on Power Systems*, vol. 24, no. 3, pp. 1523-1536, Aug. 2009.
  [7] X. Xu, H. Jia, H. Chiang et al., "Dynamic modeling and interaction of
- [7] X. Xu, H. Jia, H. Chiang et al., "Dynamic modeling and interaction of hybrid natural gas and electricity supply system in Microgrid," *IEEE Transactions on Power Systems*, vol. 30, no. 3, pp. 1212-1221, May 2015.
- [8] C. He, C. Dai, L. Wu et al., "Robust network hardening strategy for enhancing resilience of integrated electricity and natural gas distribution systems against natural disasters," *IEEE Transactions on Power Systems*, vol. 33, no. 5, pp. 5787-5798, Sept. 2018.
  [9] M. Shahidehpour, Y. Fu and T. Wiedman, "Impact of natural gas infra-
- [9] M. Shahidehpour, Y. Fu and T. Wiedman, "Impact of natural gas infrastructure on electric power systems," *Proceedings of the IEEE*, vol. 93, no. 5, pp. 1042-1056, May 2005.
- [10] K. Pambour, B. Erdener, R. Bolado-Lavin et al., "SAInt a novel quasi-dynamic model for assessing security of supply in coupled gas and electricity transmission networks," Applied Energy, vol. 203, pp. 829-857, Oct. 2017.
- [11] R. Levitan, S. Wilmer, and R. Carlson, "Unraveling gas and electric interdependencies across the eastern interconnection," *IEEE Power and Energy Magazine*, vol. 12, no. 6, pp. 78-88, Nov.-Dec. 2014.
- [12] M. Shariatkhah, M. Haghifam, G. Chicco et al., "Adequacy modeling and evaluation of multi-carrier energy systems to supply energy services from different infrastructures," *Energy*, vol. 109, no. 1, pp. 1095-1106, Aug. 2016.
- [13] S. Chen, Z. Wei, G. Sun et al., "Multi-linear probabilistic energy flow analysis of integrated electrical and natural-gas systems," IEEE Trans-

- actions on Power Systems, vol. 32, no. 3, pp. 1970-1979, May 2017.
- [14] T. Li, M. Eremia, and M. Shahidehpour, "Interdependency of natural gas network and power system security," *IEEE Transactions on Power Systems*, vol. 23, no. 4, pp. 1817-1824, Nov. 2008.
- [15] M. Chertkov, S. Backhaus, and V. Lebedev, "Cascading of fluctuations in interdependent energy infrastructures: gas-grid coupling," *Applied Energy*, vol. 160, pp. 541-551, Dec. 2015.
- [16] B. Erdener, K. Pambour, R. Lavin et al., "An integrated simulation model for analysing electricity and gas systems," *International Jour*nal of Electrical Power and Energy Systems, vol. 61, pp. 410-420, Oct. 2014.
- [17] Y. He, M. Shahidehpour, Z. Li et al., "Robust constrained operation of integrated electricity-natural gas system considering distributed natural gas storage," *IEEE Transactions on Sustainable Energy*, vol. 9, no. 3, pp. 1061-1071, Jul. 2018.
- [18] L. Bai, F. Li, H. Cui et al., "Interval optimization based operating strategy for gas-electricity integrated energy systems considering demand response and wind uncertainty," Applied Energy, vol. 167, pp. 270-279, Apr. 2016.
- [19] F. Wei, Q. Wu, Z. Jing et al., "Optimal unit sizing for small-scale integrated energy systems using multi-objective interval optimization and evidential reasoning approach," Energy, vol. 111, pp. 933-946, Oct. 2016.
- [20] A. Alabdulwahab, A. Abusorrah, X. Zhang et al., "Stochastic security-constrained scheduling of coordinated electricity and natural gas infrastructures," *IEEE Systems Journal*, vol. 11, no. 33, pp. 1674-1683, Sep. 2017.
- [21] S. Clegg and P. Mancarella, "Integrated electrical and gas network flexibility assessment in low-carbon multi-energy systems," *IEEE Transactions on Sustainable Energy*, vol. 7, no. 2, pp. 718-731, Apr. 2016
- [22] M. Carlos and S. Pedro, "Integrated power and natural gas model for energy adequacy in short-term operation," *IEEE Transactions on Pow*er Systems, vol. 30, no. 6, pp. 3347-3355, Nov. 2015.
- [23] L. Bai, F. Li, T. Jiang et al., "Robust scheduling for wind integrated energy systems considering gas pipeline and power transmission N-1 contingencies," *IEEE Transactions on Power Systems*, vol. 32, no. 2, pp. 1582-1584, Mar. 2017.
- [24] J. Fang, Q. Zeng, X. Ai et al., "Dynamic optimal energy flow in the integrated natural gas and electrical power systems," *IEEE Transactions on Sustainable Energy*, vol. 9, no. 1, pp. 188-198, Jan. 2018.
- [25] Z. Bao, D. Chen, L. Wu et al., "Optimal inter- and intra-hour scheduling of islanded integrated-energy system considering linepack of gas pipelines," Energy, vol. 171, no. 1, pp. 326-340, Mar. 2019.

Zhejing Bao received her B.S., M.S., and Ph.D. degrees in control science and engineering from Shandong University, Jinan, China, in 1996 and 1999, and Zhejiang University, Hangzhou, China, in 2007, respectively. Afterwards, she worked as a Postdoctoral Research Associate at the College of Electrical Engineering, Zhejiang University from 2007 to 2009. She is currently an Associate Professor with Zhejiang University. Her research interests include the modelling, coordinated scheduling optimization and intelligent control of multi-energy systems.

Qihong Zhang received his B.S. degree in electrical engineering from Zhejiang University, Hangzhou, China, in 2017. Currently, he is working toward the master degree with the College of Electrical Engineering in Zhejiang University. His research interests include the failure propagation mechanism in integrated electricity and natural gas systems.

Lei Wu received the B.S. degree in electrical engineering and the M.S. degree in systems engineering from Xi'an Jiaotong University, Xi'an, China, in 2001 and 2004, respectively, and the Ph.D. degree in electrical engineering from the Illinois Institute of Technology (IIT), Chicago, USA, in 2008. He was a Senior Research Associate with the Robert W. Galvin Center for Electricity Innovation, IIT from 2008 to 2010. He worked as summer Visiting Faculty at NYISO in 2012. He was a Professor with the Electrical and Computer Engineering Department, Clarkson University, Potsdam, USA till 2018. Currently, he is an Associate Professor with the Electrical and Computer Engineering Department, Stevens Institute of Technology, Hoboken, USA. His research interests include power systems operation and planning, energy economics, and community resilience microgrid.

**Dawei Chen** received his B.S. degree in electrical engineering from Zhejiang University, Hangzhou, China, in 2016. Currently, he is working toward the Ph.D. degree with the College of Electrical Engineering in Zhejiang University. His research interests include the coordinated optimization and control of the multi-energy systems.